

Distribuzione dimensionale, solubilità e rapporti caratteristici delle aree sorgente di marker di polveri sahariane nel PM10 campionato all'isola di Lampedusa

S. Becagli¹, D. M. Sferlazzo², F. Anello³, C. Bommarito³, G. Calzolai⁴, M. Chiari⁴, A. di Sarra⁵, D. Frosini¹, J.L. Gómez-Amo⁵, F. Lucarelli⁴, M. Marconi¹, D. Meloni⁵, F. Monteleone³, S. Nava⁴, G. Pace⁵, M. Severi¹, R. Traversi¹ and R. Udisti¹.

¹ Dipartimento di Chimica, Università di Firenze, Via della Lastruccia 3, 50019 Sesto Fiorentino, Italy

² ENEA, Laboratory for Earth Observations and Analyses, I-92010 Lampedusa, Italy

³ ENEA, Laboratory for Earth Observations and Analyses, I-90141 Palermo, Italy

⁴ Dipartimento di Fisica e Astrofisica, Università di Firenze, Via Sansone 1, 50019 Sesto Fiorentino, Italy

⁵ ENEA, Laboratory for Earth Observations and Analyses, S. Maria di Galeria, I-00123 Roma, Italy

silvia.becagli@unifi.it

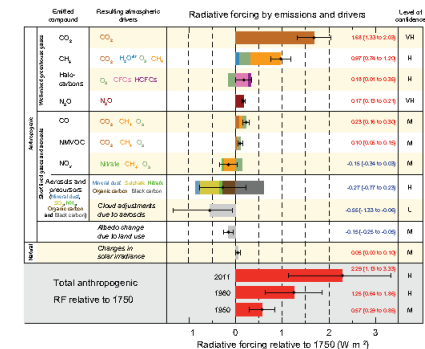


PM2014 - GENOVA

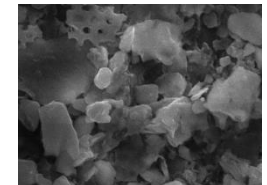
Importance of the study on Saharan dust aerosol

Sahara is the largest source of soil-derived aerosols, with an annual emission estimated to be about 600 Tg yr⁻¹ (D'Almeida, 1986; Marticorena et al, 1997). Dust may also greatly increase the atmospheric levels of PM, adversely affecting air quality.

Mineral aerosols affect the atmospheric radiative balance through scattering, absorption, and emission of radiation (IPCC, 2013; di Sarra et al., 2011); they also affect it indirectly, by acting as cloud condensation nuclei (Levin et al., 1996) and modifying cloud properties.



Dust particles frequently act as reaction surfaces for reactive gases (Dentener et al., 1996; Levin et al., 1996), affecting atmospheric chemical processes.



Mediterranean marine regions are highly influenced by crustal dust deposition, which may provide large amounts of nutrients for phytoplankton (Béthoux et al., 1996; Guerzoni et al., 1999).



NASA/MODIS



$35.5^{\circ}\text{N}, 12.6^{\circ}\text{E}$

meteorological station and air inlet for
CO₂, CH₄, N₂O, CFCs, HFCs, HCFC measurements

<http://www.lampedusa.enea.it/>

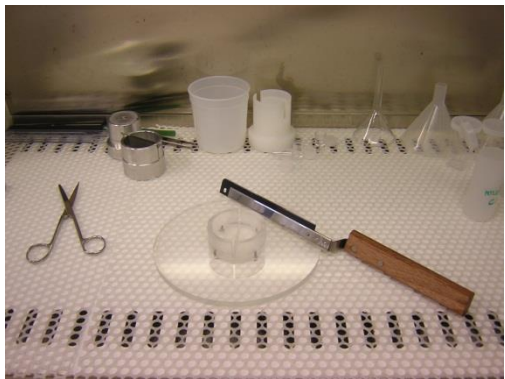


Aerosol sampling Campaigns



- ✓ Jun 04 – Dec 06:
PM10 - PM2.5 -
PM1 alternatively
- ✓ Jan 2007- today:
PM10.
- ✓ Spr-Sum 06:
campaign with 8
stages impactor
- ✓ Jan 10: sampling
also on quartz
filters for EC/OC.

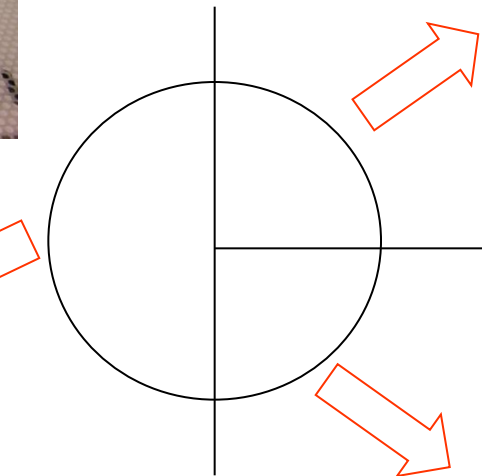
Cutting in clean conditions



Dept. of Chemistry, Univ. of Florence

Ions Chromatography
 Na^+ , NH_4^+ , K^+ , Mg^{2+} , Ca^{2+} ,
 Cl^- , NO_3^- , SO_4^{2-} , MSA, Ac,
For, Gly, Ox

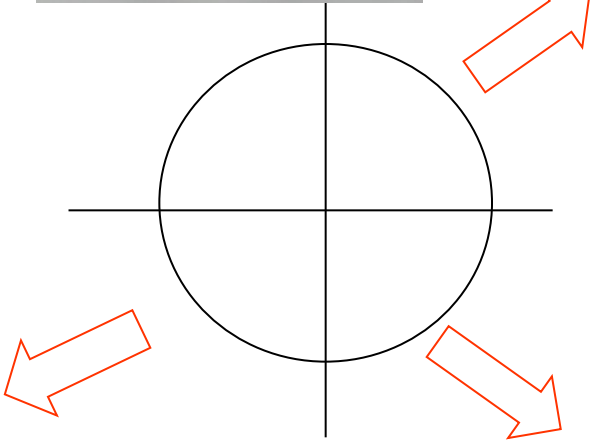
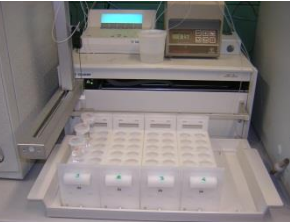
PIXE: elements
total content



ICP AES HNO_3
pH 1.5

Al, Cd, Ba, Pb,
Si, Ti, V, Cr, Mn,
Fe, Ni, Cu, Zn,
As, Mo

Dept. of Physics and INFN



Ions Chromatography
 Na^+ , NH_4^+ , K^+ , Mg^{2+} , Ca^{2+} ,
 Cl^- , NO_3^- , SO_4^{2-} , MSA, Ac,
For, Gly, Ox

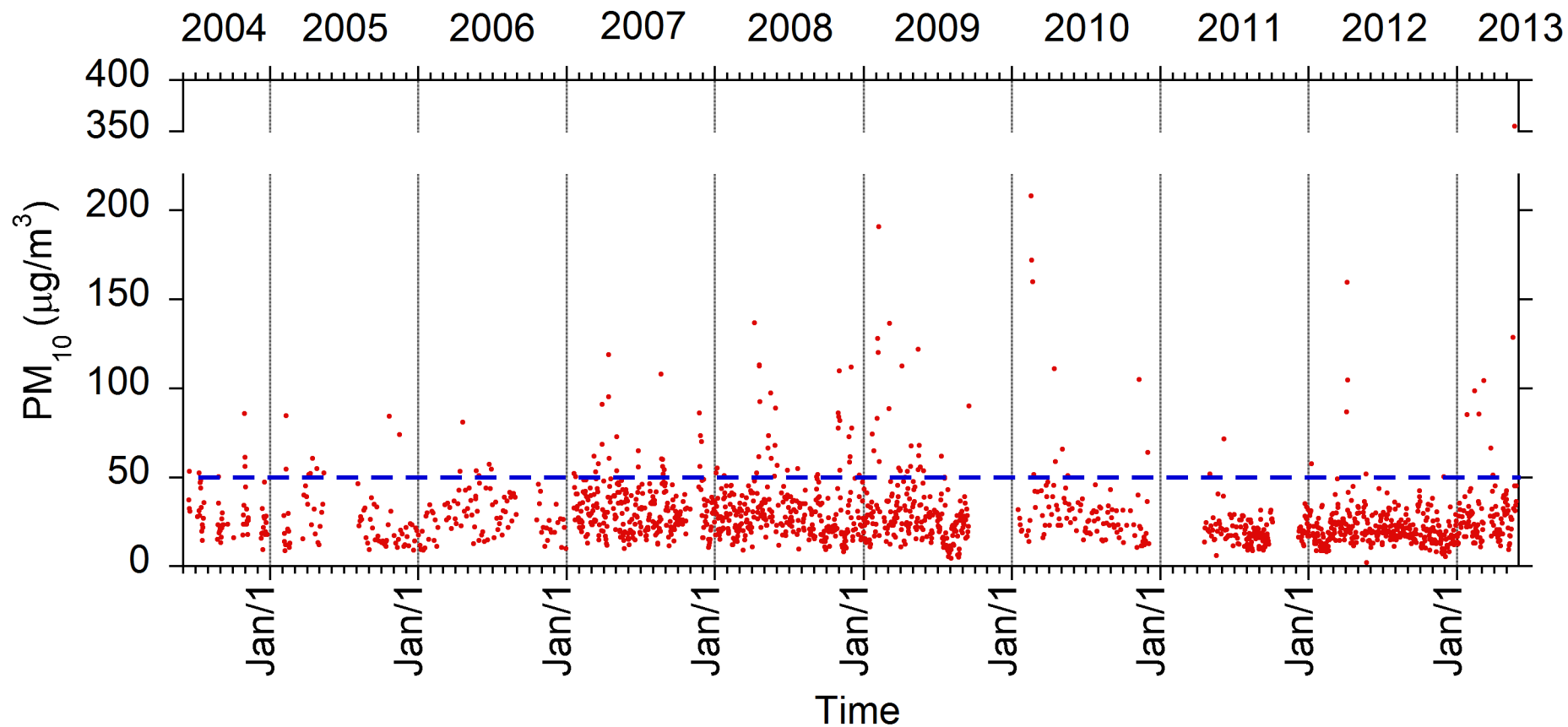
ICP AES $\text{HNO}_3\text{-H}_2\text{O}_2$

Al, Cd, Ba, Pb,
Si, Ti, V, Cr, Mn,
Fe, Ni, Cu, Zn,
As, Mo

ICP AES HNO_3
pH1.5

Al, Cd, Ba, Pb,
Si, Ti, V, Cr, Mn,
Fe, Ni, Cu, Zn,
As, Mo





Crustal aerosol =

$$1.89 * \text{Al} + 2.14 * \text{Si} + 1.4 * \text{nssCa} + 2.12 * \text{Fe} + 1.35 * \text{nssNa} + \\ 1.66 * \text{nssMg} + 1.21 * \text{nssK} + 1.67 * \text{Ti}$$

$$\text{tot Na} = \text{nssNa} + \text{ssNa}$$

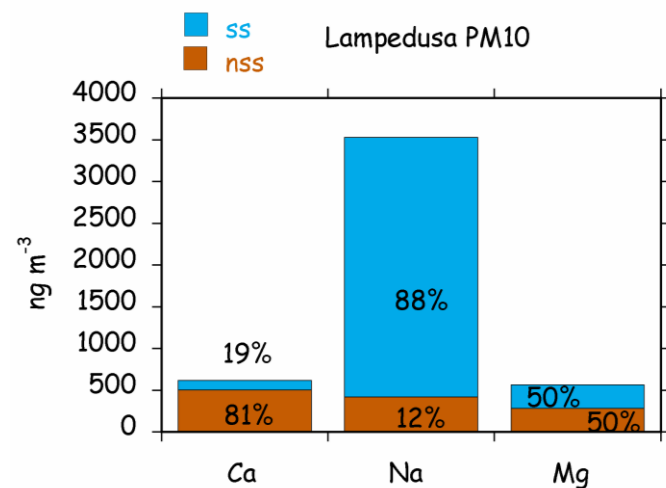
$$\text{tot Ca} = \text{nssCa} + \text{ssCa}$$

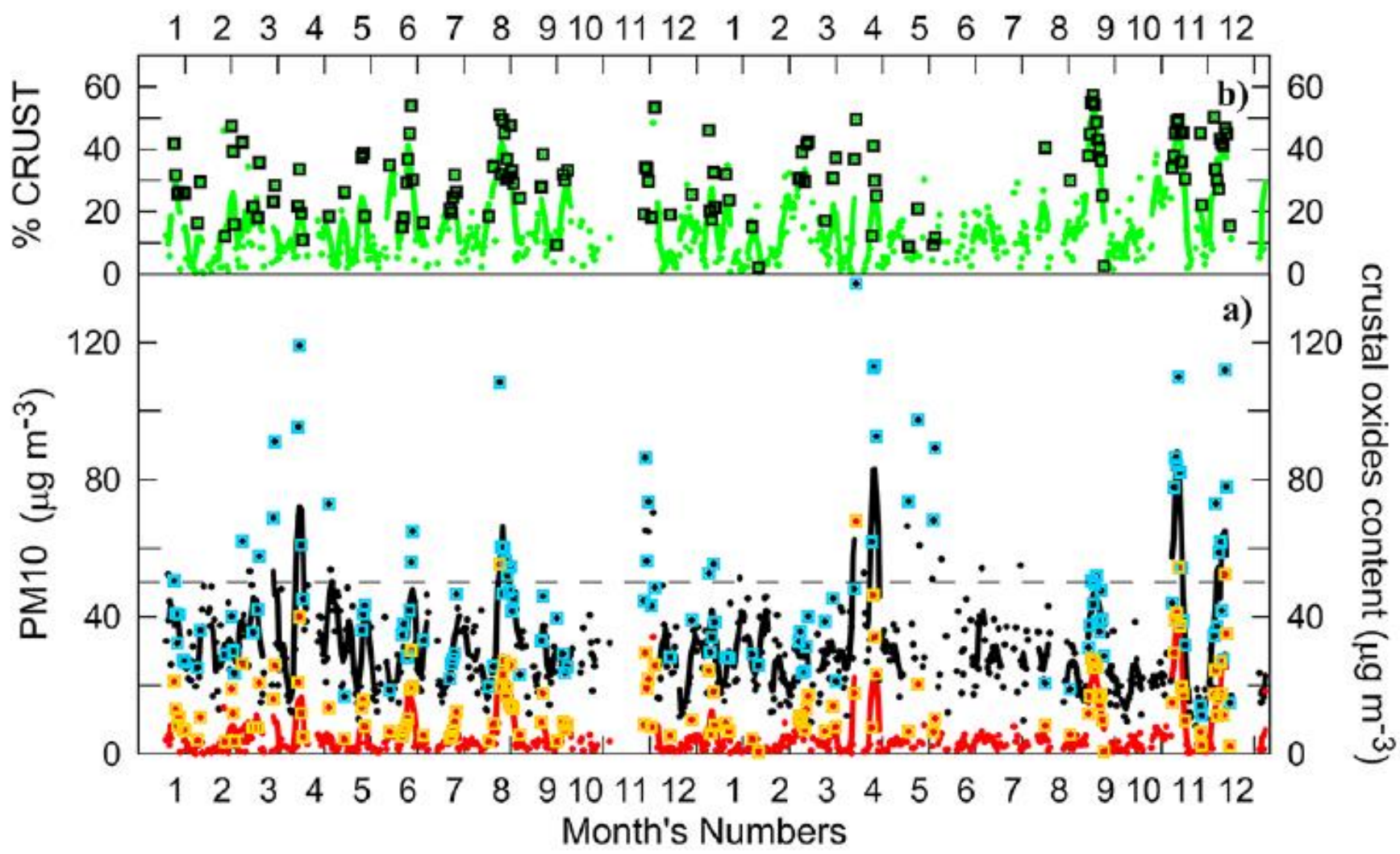
$$\text{ssNa} = \text{tot Na} - (\text{Na/Ca})_{\text{crust}} * \text{nssCa}$$

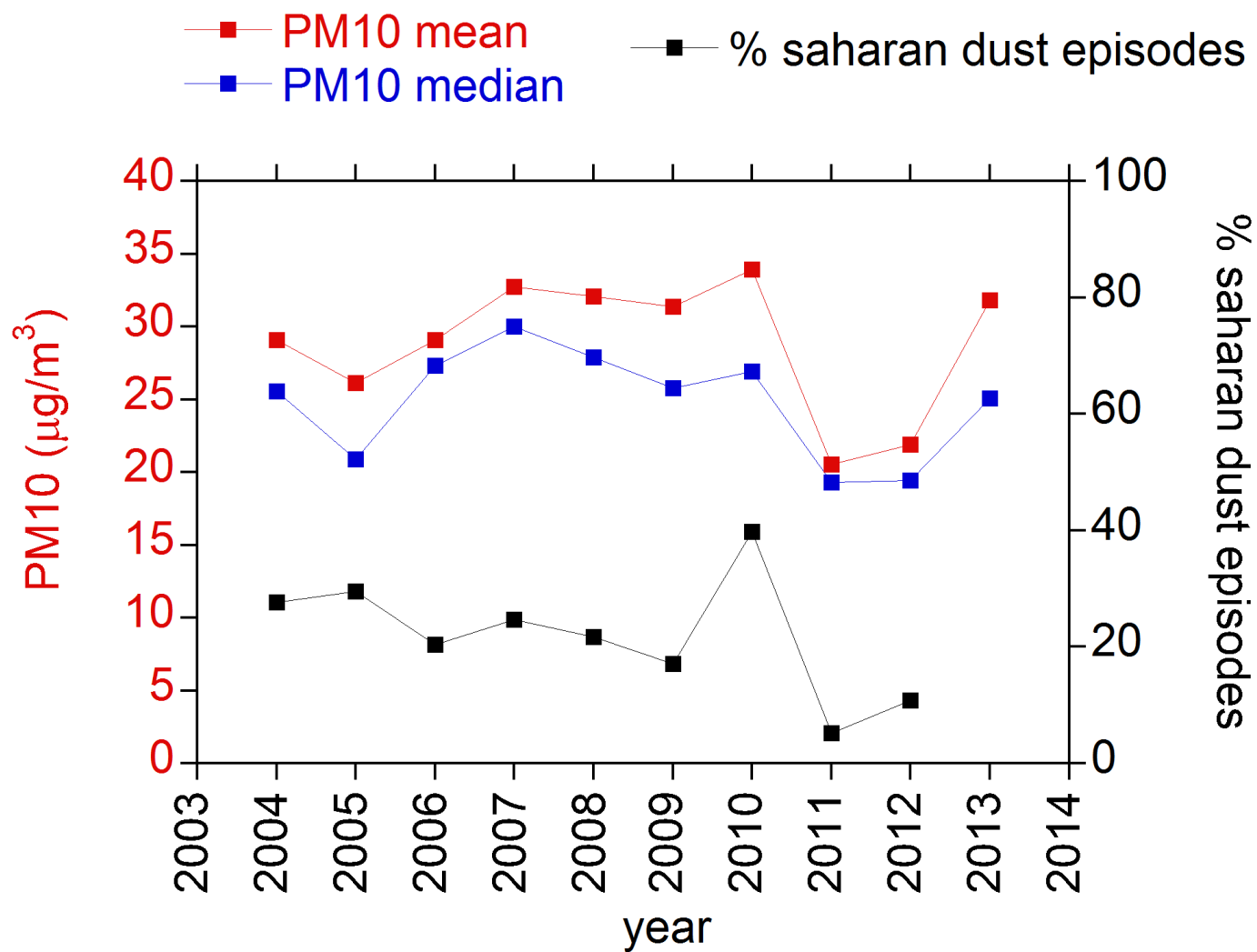
$$\text{nssCa} = \text{tot Ca} - (\text{Ca/Na})_{\text{sea water}} * \text{ssNa}$$

$$(\text{Ca/Na})_{\text{sea water}} = 0.038 \text{ w/w}$$

$$(\text{Na/Ca})_{\text{crust}} = 0.569 \text{ w/w}$$

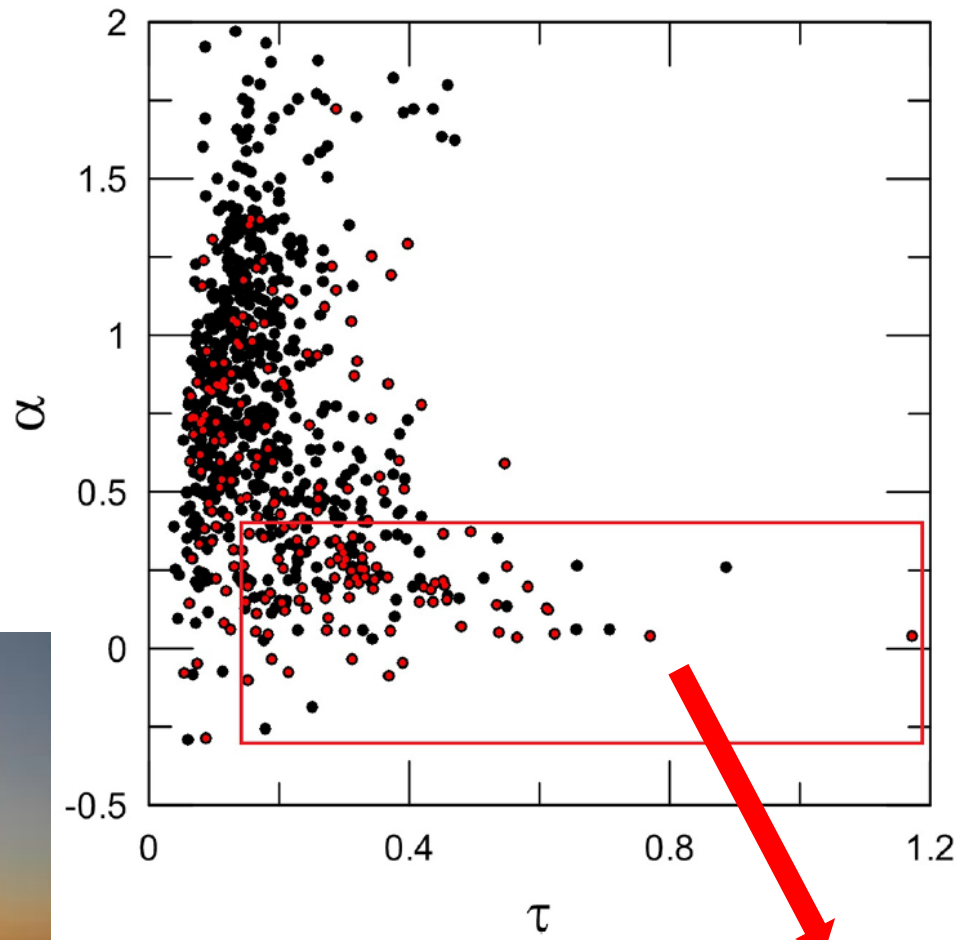






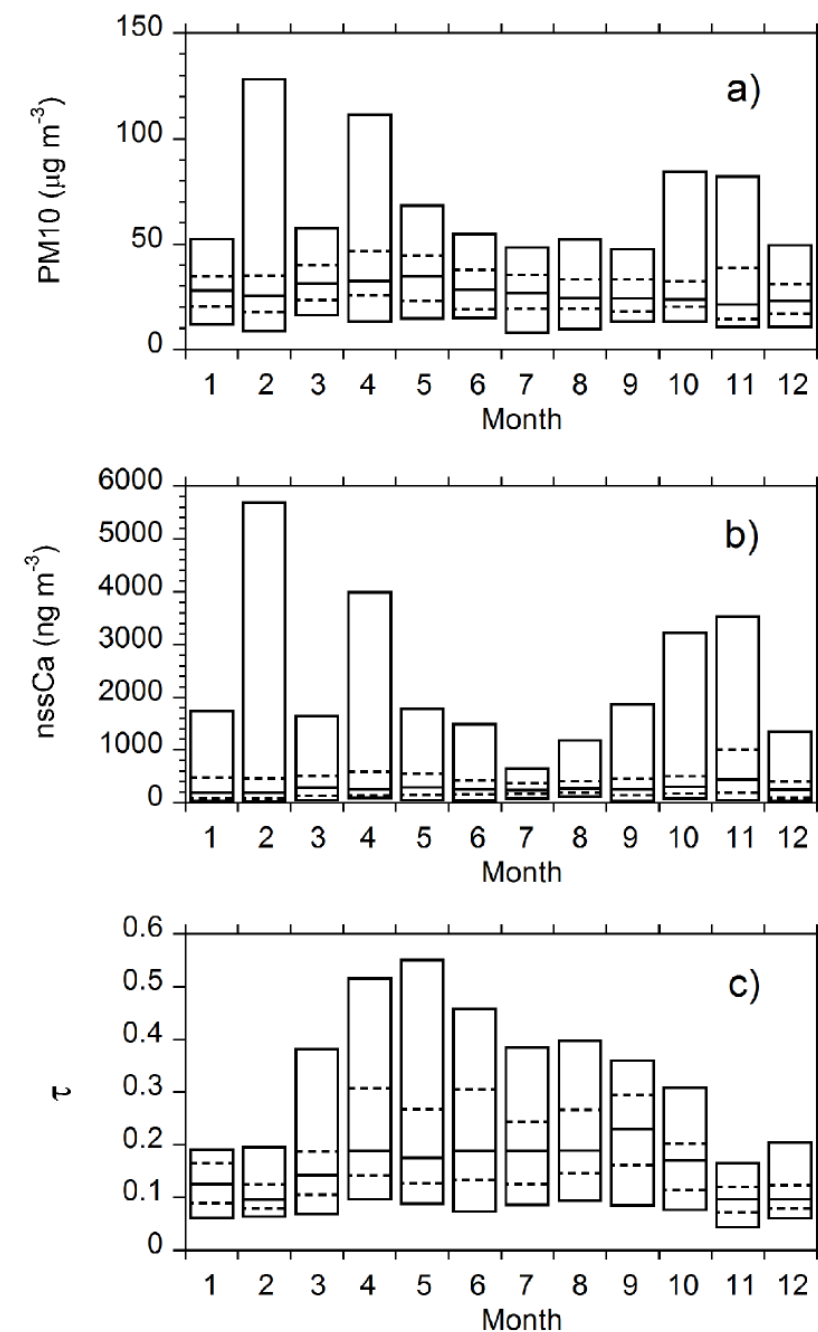
● Eventi sahariani al suolo

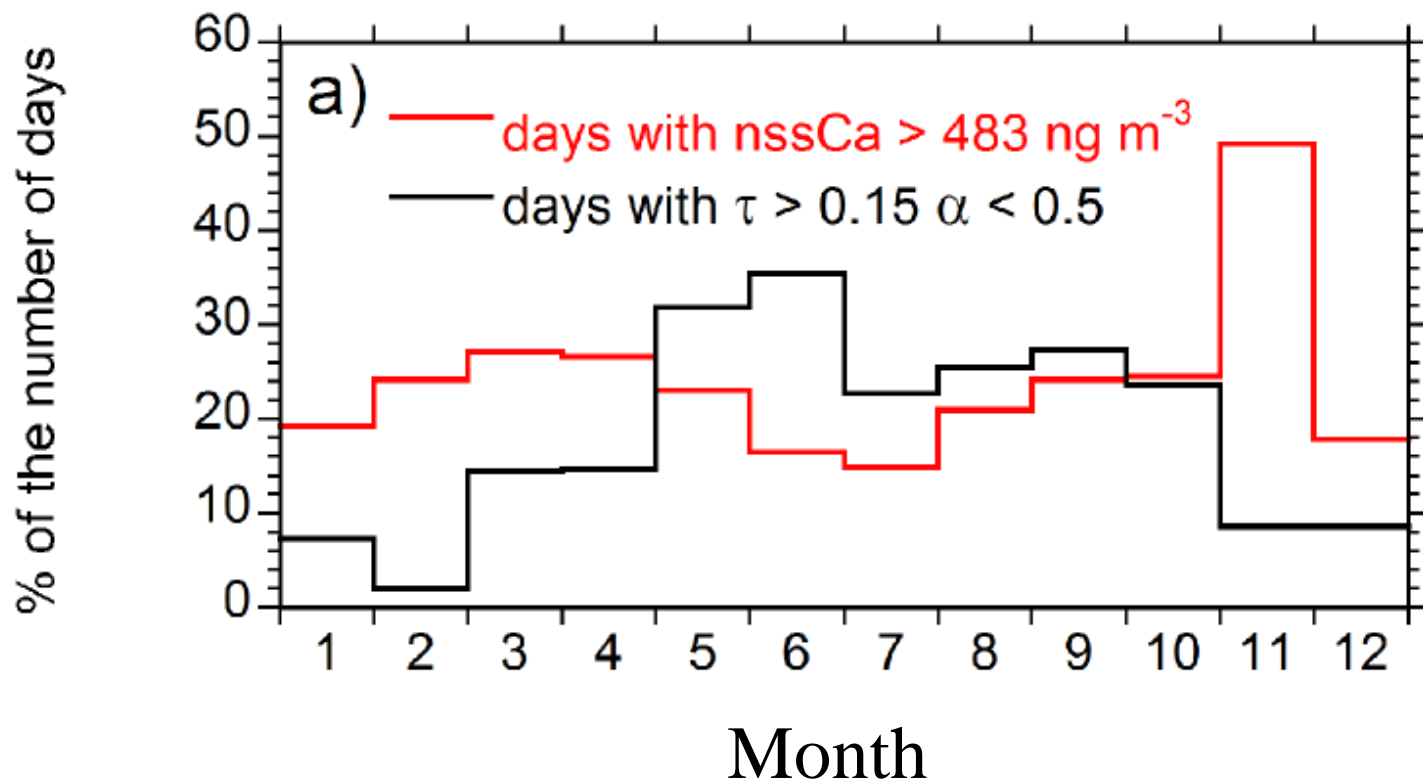
$$\alpha = -\frac{\ln(\tau_{415.6}/\tau_{868.7})}{\ln(415.6/868.7)}$$



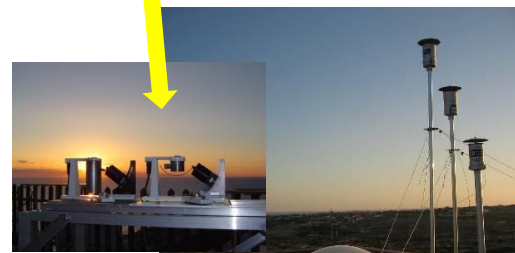
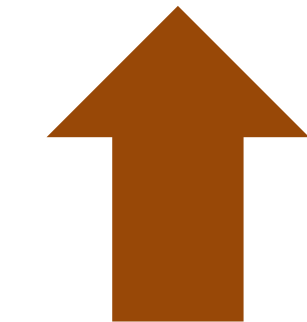
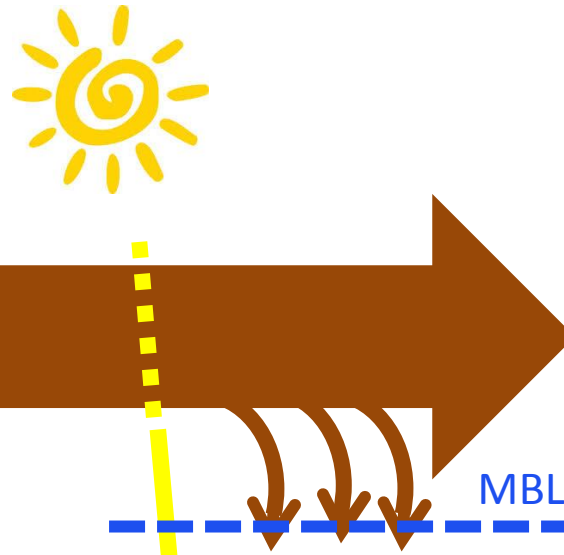
Eventi sahariani
(Pace et al. 2006)



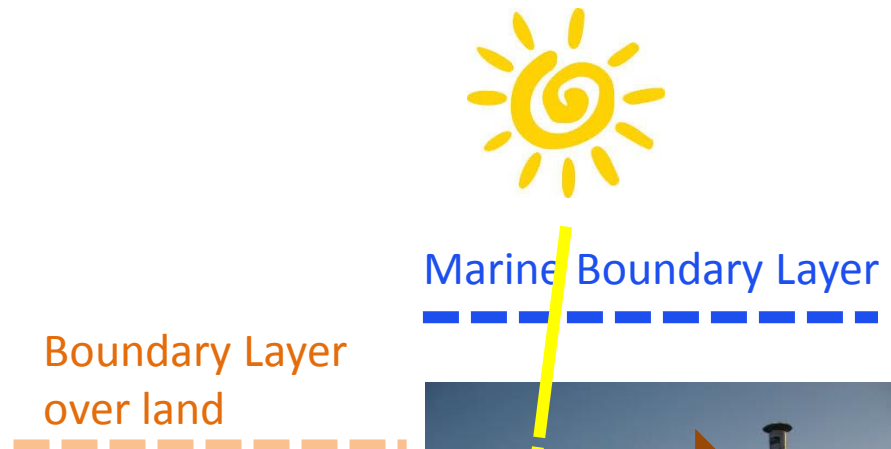




Summer



Winter





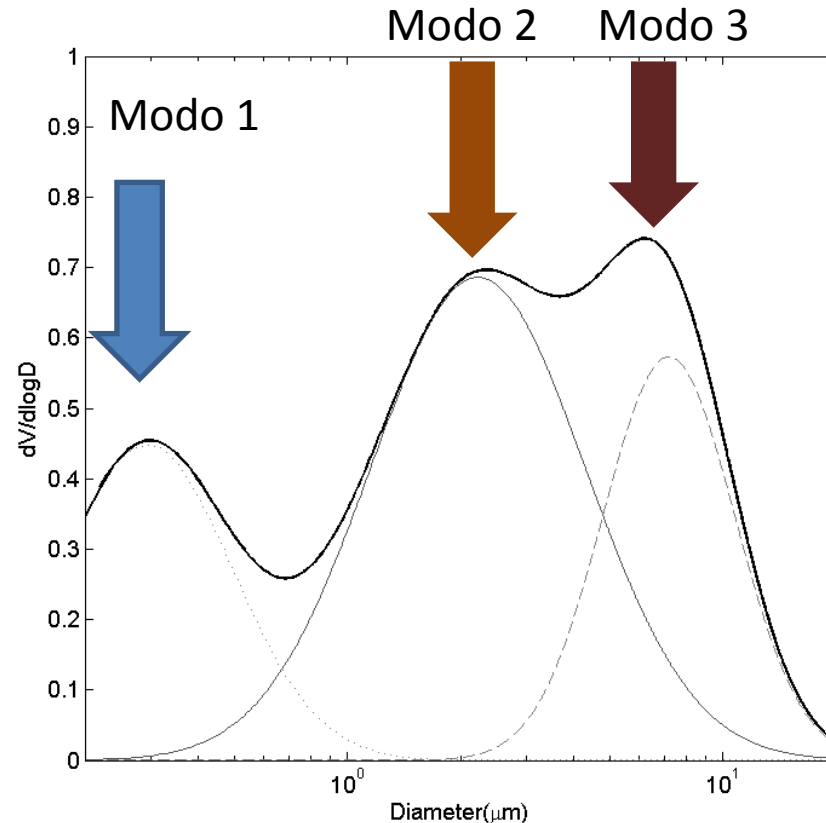
Distribuzione
dimensionale e
solubilità

PM10 bulk

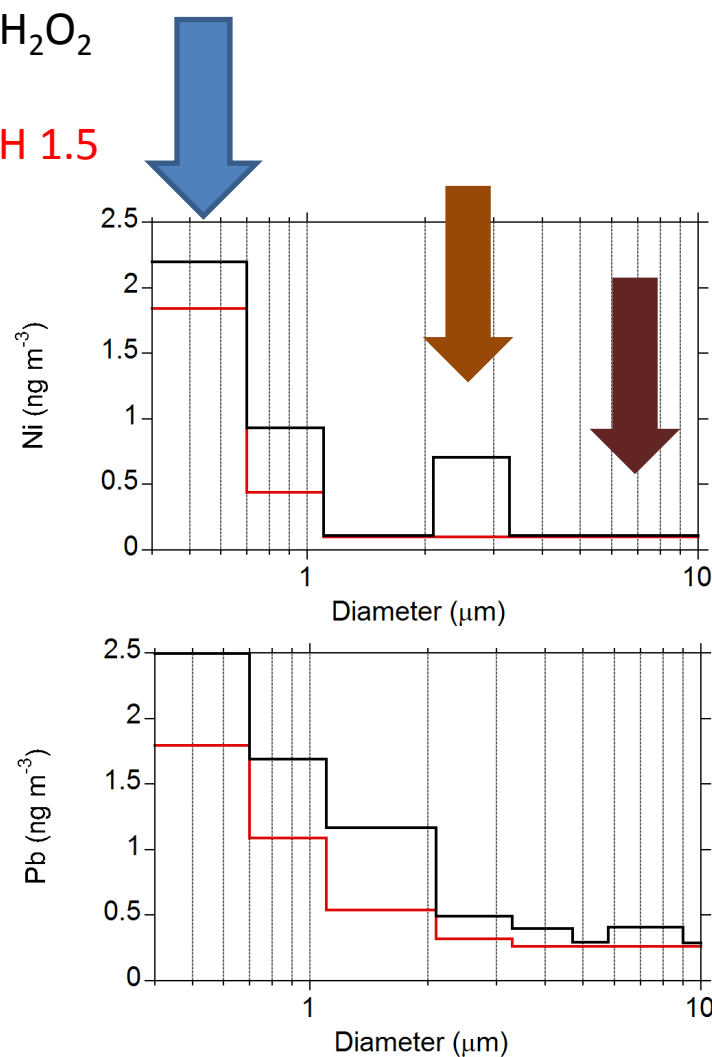
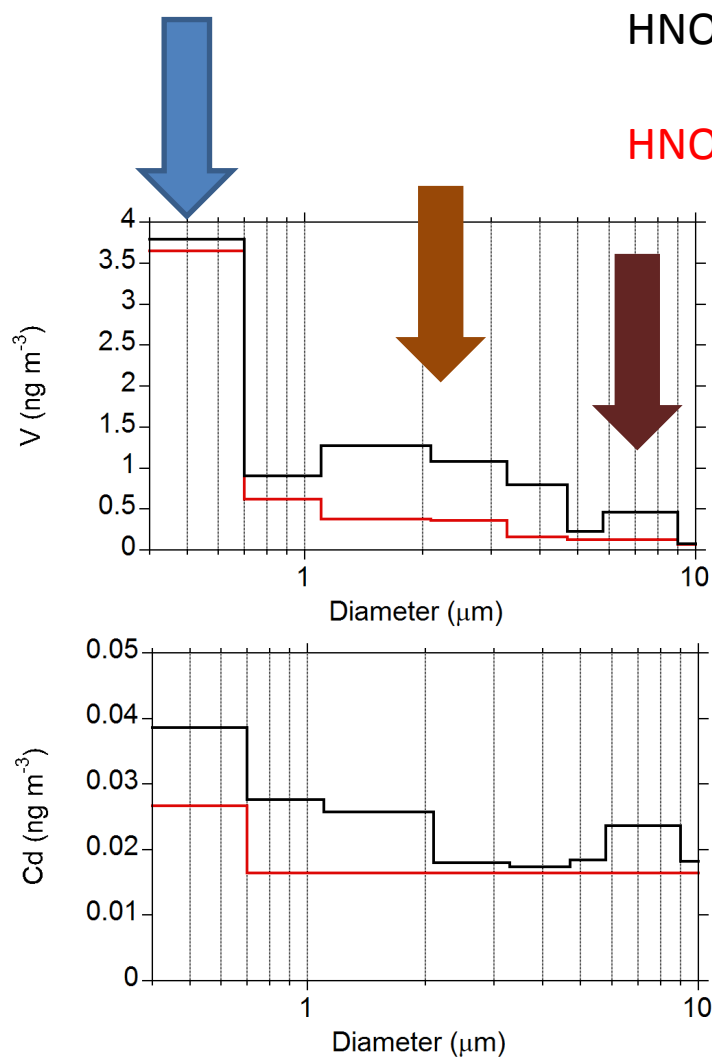
Solubilità $\text{HNO}_3 \text{ pH1.5 } \% = 100 * \frac{\text{Me}_{\text{HNO}_3 \text{ pH1.5}}}{\text{Me}_{\text{PIXE}}}$

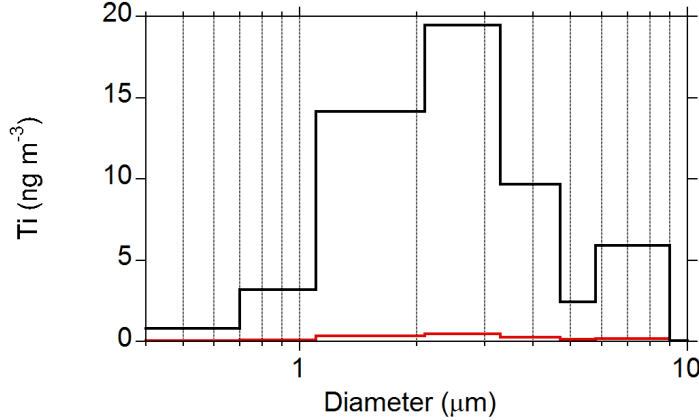
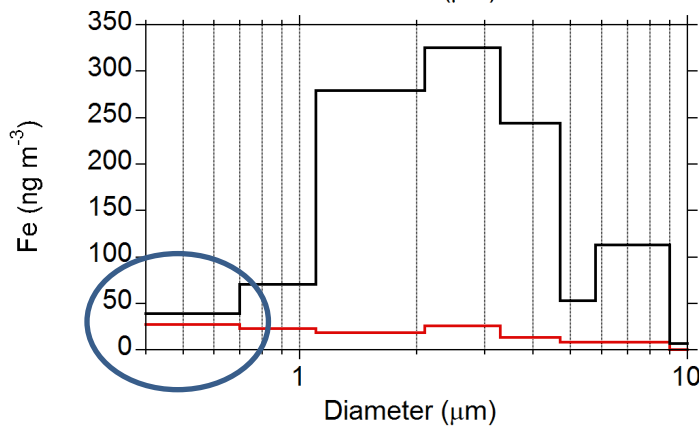
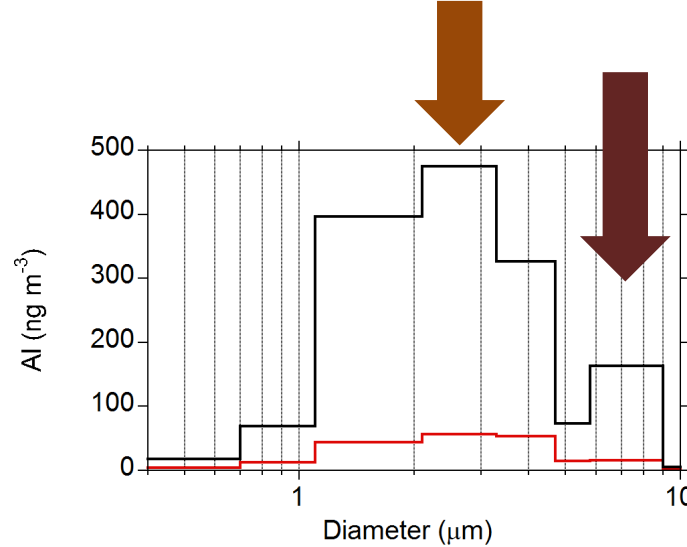
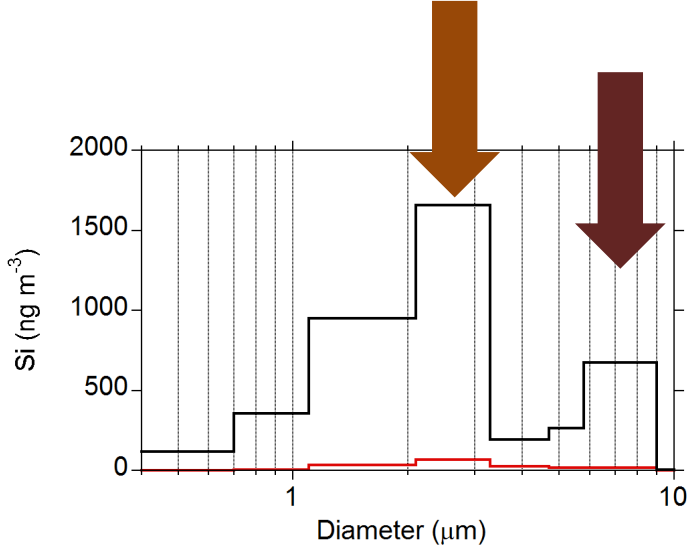
	Saharan dust event				Non Saharan dust events			
	Median	Mean	Std dev of the mean	N. valid data	Median	Mean	Std dev of the mean	N. valid data
Al	10.7	12.5	0.8	159	14.8	18.6	0.6	497
Fe	5.9	7.5	0.4	158	13.0	15.3	0.5	499
Ca	75.8	75.2	1.5	163	76.8	76.4	1.0	495
Mg	75.4	73.4	2.5	147	91.7	87.1	1.4	395
K	39.5	40.5	1.3	166	63.7	63.0	0.9	510
Mn	54.6	53.9	1.2	153	54.9	55.2	1.1	330
V	46.6	46.7	2.1	104	66.7	65.1	1.5	295
Ni	50.9	50.7	2.1	136	63.0	61.3	1.3	400
Cr	6.2	6.9	0.5	94	6.0	7.6	0.7	71
Cu	45.7	47.3	1.8	143	53.1	53.6	1.4	397
Pb	62.7	64.8	2.8	84	56.3	56.8	2.0	177

OPC



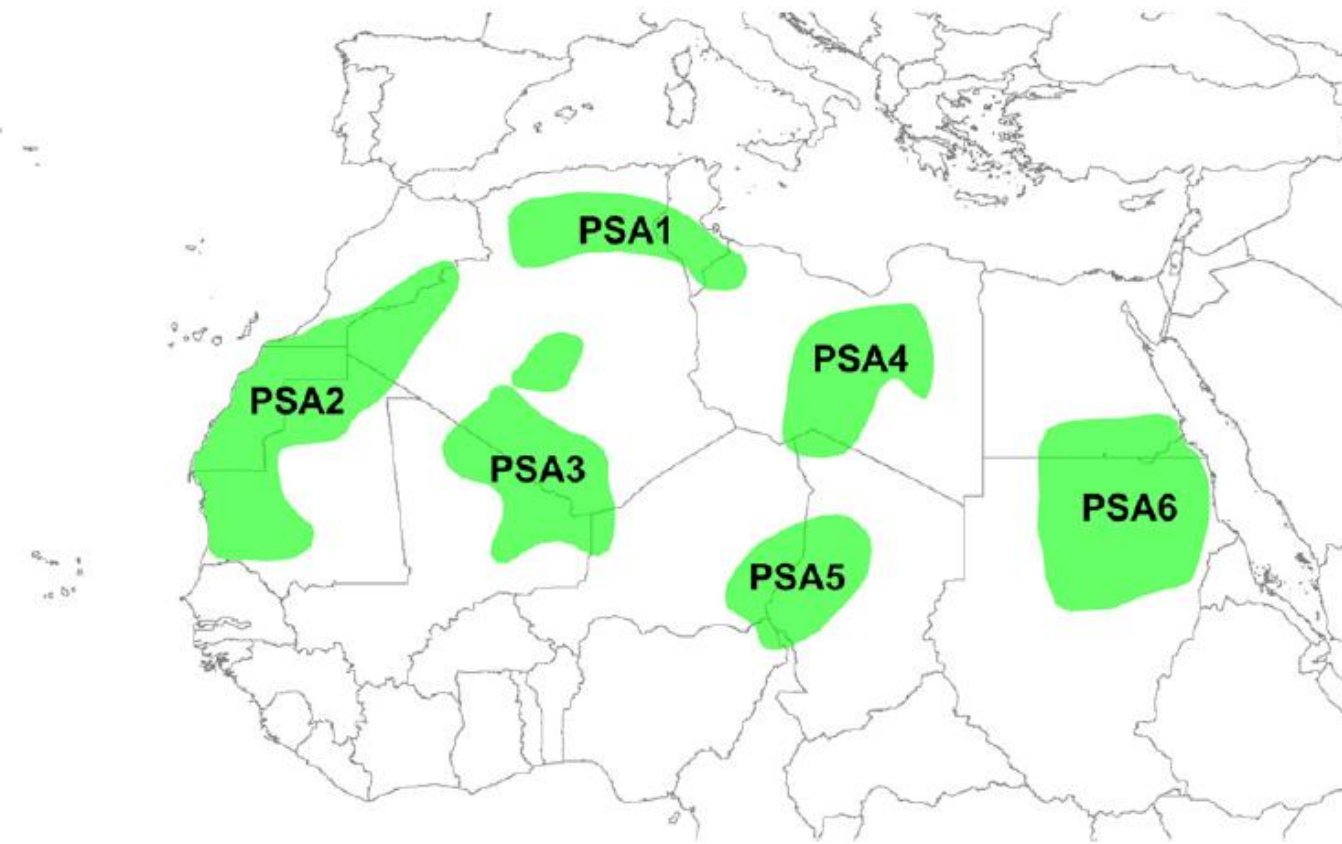
	Dv (μm)	σ	V (%)	N (%)
Mode 1	0.29	1.35	25.6	99.8
Mode 2	2.23	2.02	49.1	1.23×10^{-1}
Mode 3	7.18	1.77	25.3	1.89×10^{-3}





A satellite image of the North African region and the Mediterranean Sea. A massive, dark brown dust plume originates from the Sahara Desert in the west and extends across the central Mediterranean towards the Balkans and Eastern Europe. The dust is most concentrated in the center and east, appearing as a thick, dark band against the lighter blue of the sea. To the north, the European continent is visible with green landmasses and white cloud cover. The dust plume is particularly prominent in the middle and upper portions of the image.

Aree Sorgente



Earth-Science Reviews 116 (2013) 170–194

Contents lists available at SciVerse ScienceDirect

Earth-Science Reviews

journal homepage: www.elsevier.com/locate/earscirev



Bulk composition of northern African dust and its source sediments – A compilation
Dirk Scheuvens ^{a,b,*}, Lothar Schütz ^b, Konrad Kandler ^{a,b}, Martin Ebert ^a, Stephan Weinbruch ^a

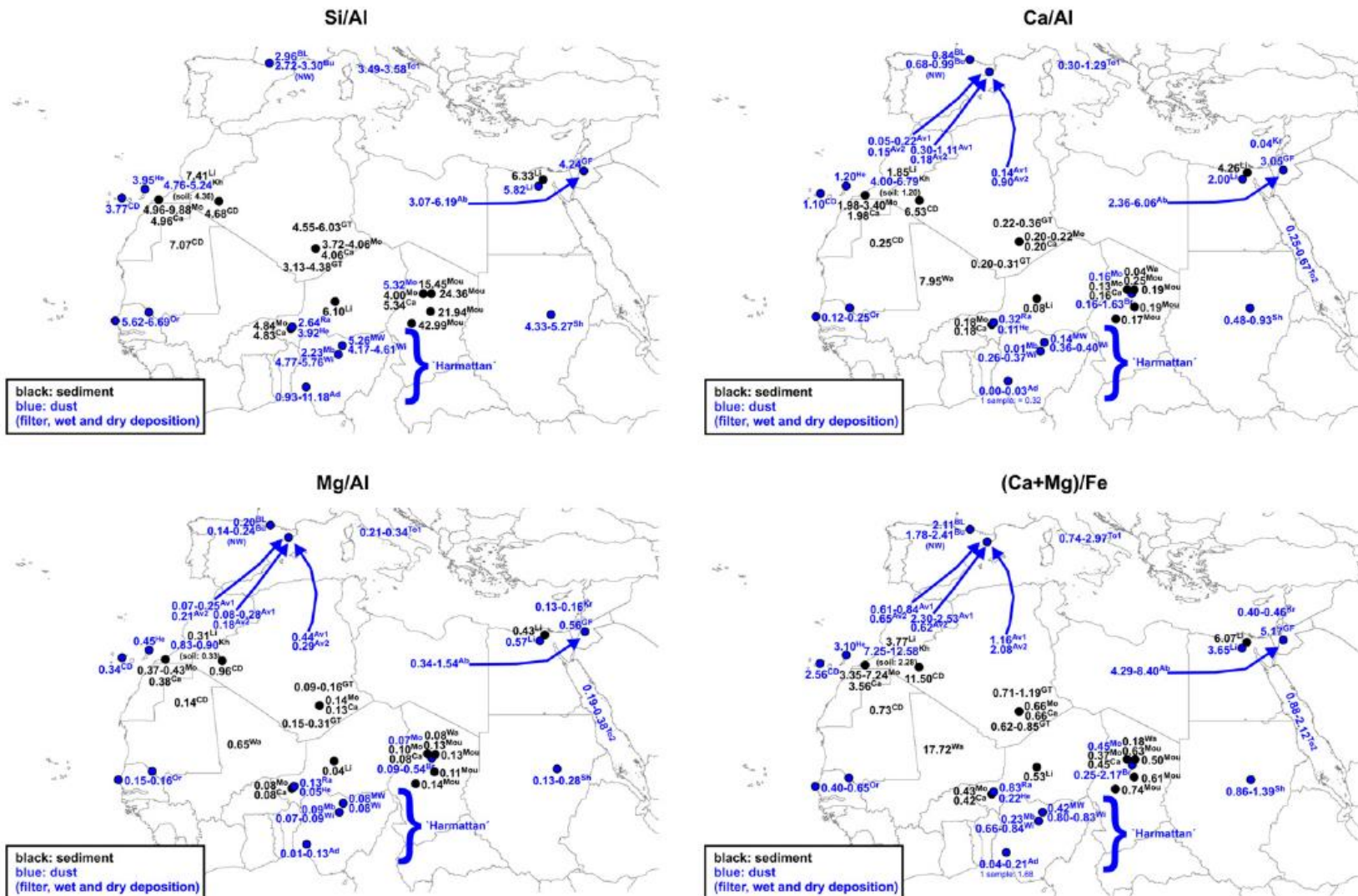


Fig. 2. Maps of northern Africa with elemental ratios of Si/Al, Ca/Al, Mg/Al, and (Ca + Mg)/Fe indices (bulk chemical analyses in wt.%) for dust and sediment samples; arrows show transport directions of mineral dust of selected studies. References: MW: McIntosh and Walker (1982), BL: Bücher and Lucas (1984), To1: Tomadin et al. (1984), Wi: Wilke et al. (1984), Ad: Adedokun et al. (1989), Bu: Bücher (1989), To2: Tomadin et al. (1989), Mb: Mäberg et al. (1991), Or: Orange et al. (1993), Sh: Sharif (1995), Gr: Ganor and Foner (1996), GT: Guiou and Thomas (1996), He: Herrmann et al. (1996), Av1: Avila et al. 1998, K: Krom et al. (1999), Gu: Guiou et al. (2002a), CD: Criado and Dorta (2003), St: Singer et al. (2003), Kb: Khirli et al. (2004), Li: Linke et al. (2005), Mo: Moreno et al. (2005), Mou: Mounkaila (2006), Av2: Avila et al. (2007), Ca: Castillo et al. (2008), Ra: Rajot et al. (2008), Ab: Abed et al. (2009), Wa: Washington et al. (2009), and Br: Bristow et al. (2010).

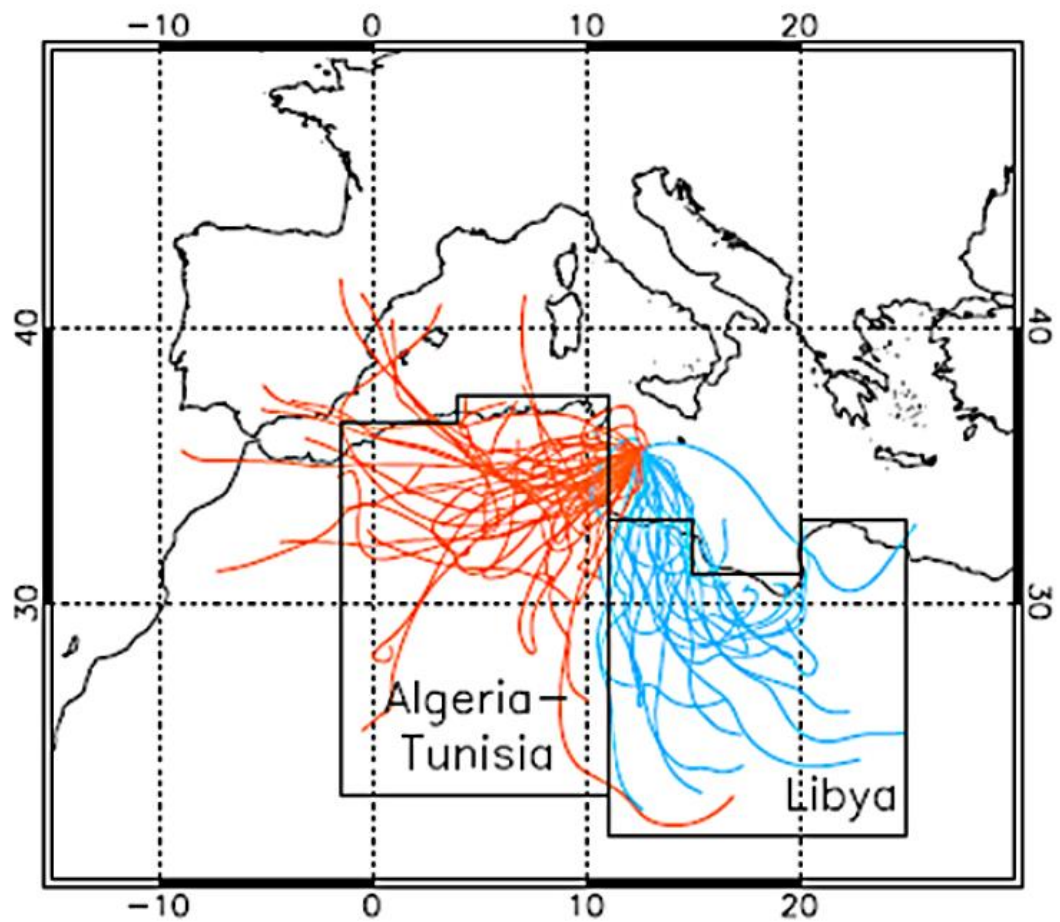
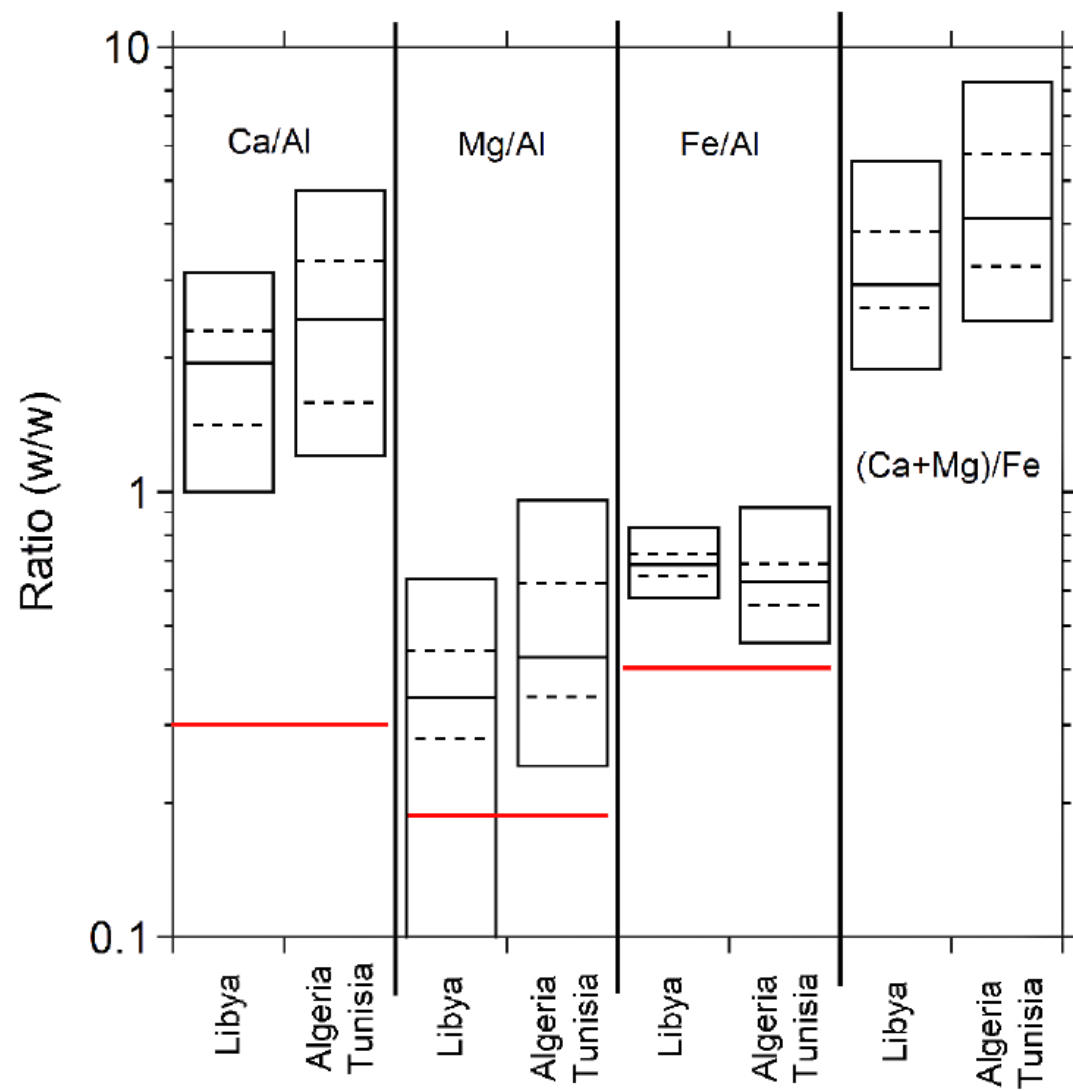


Fig. 7. Dust source regions and back trajectories fulfilling the 50 % permanence criterion for each source region (orange for Algeria-Tunisia and blue for Libya).



Conclusioni

